https://doi.org/ 10.33472/AFJBS.6.Si2.2024.3422-3528

Keloid Disease Detection using Deep Learning ResNet50 Algorithm

SHANMUGA PRIYA K[1]

Department of Computer Science and Engineering

Kongunadu College of Engineering and Technology

Trichy,India

Shanmugapriya2k1010@gmail.com

VALARMATHI P[2]

Department of Computer Science and Engineering

Kongunadu College of Engineering and Technology

Trichy,India

Valarpbvm2011@gmail.com

Abstract-A Keloid is the product of aberrant wound healing, when patients' growth states and blood perfusion vary. Keloid enlargement can be effectively inhibited by actively monitoring and treating actively forming keloids at the initial stage, which has significant medical and cosmetic ramifications. This study addresses the challenging task of inhibiting keloid enlargement through early-stage monitoring and treatment. Existing approaches utilizing Laser Speckle Contrast Imaging (LSCI) for blood perfusion determination require time- consuming manual inspection and annotation. With a focus on improving keloid growth status evaluation, this retrospective analysis incorporates intensity and blood perfusion images from 150 untreated keloid patients. The proposed model, termed the "Multi-layered Transform Architecture," introduces a cascaded vision transformer architecture, combining the strengths of vision transformers with a hierarchical approach. Additionally, the workflow incorporates a Masked Auto encoder for denoising and feature learning, and a dilated UperNet decoder. The results demonstrate noteworthy improvements across key metrics. The proposed architecture enhances the Dice coefficient by 2% for keloid segmentation, reduces perfusion unit error by 8.6 ± 5.4, decreases relative error in blood calculation by 7.8% ± 6.6%, and achieves a 1.4% increase in growth state prediction accuracy (0.927 compared to a baseline). This novel approach not only streamlines the segmentation process but also offers enhanced accuracy in predicting keloid growth states, showcasing its potential for significant medical and cosmetic implications in the early intervention and treatment of keloids.

Keywords: Multi-layered Architecture, ResNet Model, Neural Network, Deep Learning, Hierarchical Feature Extraction and Skip Connections.

1. Introductio

Keloids,which are non-cancerous tumors characterized by excessive growth of skin fibrous tissue, extend beyond the original wound limits. Common signs include raised, solid, reddish lumps or patches on the skin that may itch or sting. Despite advancements in our knowledge of collagen production and wound healing,

managing, and healing keloids pose ongoing therapeutic challenges. Pronipt detection and management of progressing keloids can **enhance both the** esthetic outcome and clinical prognosis by successfully preventing the expansion of the keloids.A method known as (LSCI) has been developed, which is based on a real-time,

non contact assessment of the decrease in speckle contrast [1]. Numerous L SCI-based investigations have been proposed to assess keloids' blood perfusion [2,3]. These studies reveal that blood- perfusion concentrations in keloids are much greater than in neighbouring regular skin tissues as well as those that are not, suggesting that keloids are growing. However, the semi- automatic LSCI-based blood-flow tracking system in clinical settings still has some problems [4]. The problem of missing labeling and mislabeling is particularly serious when blood flow from several keloids with uneven borders and abnormal skin pigmentation is detected.Thanks to deep learning's explosive expansion, computer vision modeling algorithms now have high identification capacity for medical imagery [5]. Notably, deep learning is frequently utilized in dermatology and plastic surgery to study skin with good performance, including diagnosing benign and malignant melanoma [6], discriminating numerous skin illnesses [7], and evaluating burn regions [8]. Nevertheless, the assessment of the literature does not yield any pertinent studies on prognosis prediction and keloid evaluation.The aim of this research is to construct a deep learning-driven workflow, integrate diverse DL and machine learning designs, bridge the gaps between upstream and downstream tasks, and provide supplementary usage opportunities.

The following is a description of the principal research contributions:

Characteristics from upstream and downstream are encoded and concatenated using a recently constructed cascaded vision converter design.A proposed automated workflow that includes keloid division, blood-perfusion estimation, and prognosis prediction is made for the clinical evaluation of keloids.It performs better when compared to conventional convolution neural networks. **2. Related Work**

There are not many studies on keloid evaluation, particularly when it comes to LSCI-based blood perfusion. This section mostly reviews the most recent and earlier research on skin lesions. This section also introduced similar deep-learning techniques.

2.1. Segmentation task over skin injury

In recent times, CNN has been lengthily employed for skinlesion division, with most of these studies having a U-shaped architecture [9]. As an illustration, author suggested a deep mixed convolutional network that was based on Efficient Net and U Net++ [10].

Numerous studies have attempted to incorporate attention blocks into the network rather than altering the U-shaped topology. To identify skin lesions, researcher developed a response attentiveness network built on an ambient encoder network [11]. For the highly interconnected convolution network, a novel work was presented with a different attention block called the channel spatially fast attention-guided filter [12]. To improve the characteristics obtained for up sampling procedures. [13] suggested an adaptive dual focus module.

2.2. Classification task over skin injury

The primary challenge frequently encountered in computer vision is categorization, and numerous methods have emerged since the introduction of Image Net [14]. In a study [15]. skin lesions were categorized into multiple classes through a machine learning approach coupled with a hybrid selection of deep features. Utilized the skewness-controlled Support Vector Regression(SVR) technique to pinpoint optimal features for classifying various types of skin lesions. This involved extracting features using ResNet50 and ResNet 101 [16] Rather of using deep learning approaches, [17] employed a combination of machine learning techniques. According to [18],a novel multi-weight loss function may be used to classify skin lesions on an imbalanced small database.

2.3. Integration of classification and segmentation

Several techniques have been developed that combine classification and segmentation into a single framework, as opposed to segmenting and classifying independently. Manzoor suggested using CNN and features fusion in a lightweight manner [19]. And also classified benign and malignant cancer by using anedge approach to section the lesion using AlexNet and VGG16 for feature extraction. [20] presented an integrated system for the identification and recognition of skin lesions that incorporates CNN models and machine learning. The experiments classification accuracies were raised by combining both segmentation and classification into a single framework.

2.4. Research gaps identified

- Research on keloid evaluation, particularly in LSCI-based blood perfusion analysis, is lacking. Keloids' abnormal wound healing and development states demand particular attention that present literature lacks.

- Convolutional neural networks (CNNs) with U-shaped architectures are routinely used for skin lesion segmentation, although research is lacking on their effectiveness for keloid segmentation. Keloids are irregularly shaped and grow in different ways. thus segmentation methods for them must be carefully examined.

Research on skin lesion categorization methods lacks specificity on keloid classification problems. Keloids are a separate subclass of skin lesions, and defining them requires a better understanding of their distinctive traits, which is not sufficiently covered in the literature.Integrated classification and segmentation algorithms for skin lesion analysis have been studied, but their effectiveness for keloid images is still unclear. Keloid evaluation requires a holistic approach that considers spatial extent (segmentation) and growth status (classification), requiring specialist research on keloids' integration issues.

3. Proposed framework for early stage keloid prediction 3.1.

Samples for the study

We retrospectively included patients with keloids found at Dhanam Homeo Clinic, Musiri in 2019 and 2021 developed the flow chart. The following patients met the inclusion criteria: (1) those who had at least one keloid; (2) those who had color bloodperfusion images and stored black-and-white intensity images from LSCI; (3) those who had not received prior treatment; (4) those who had no systemic disease; and (5) those who had continuation data. Following screening, keloids were gathered from seven different areas: the back, chest, ear, face, hip, leg, and abdomen. The study enrolled 150 individuals.

3.2. Manual and Device Annotations

LSCI (PeriCam PSI System®; Perimed, Järfälla, Sweden) was used to measure keloid perfusion, and PimSoft 1.2.2.00, a manufacturer's program, was used for image processing.The

software generated an intensity image and a blood-perfusion image for the scanned region. Images of the patients' blood perfusion and intensity were gathered. Blood perfusion was measured and reported in terms of perfusion units (PUs, mL/100 g/min). Using the "labelme" program, two plastic surgeons individually tagged the intensity photographs. Every unedited image was divided into two tissue categories: background (nonkeloid) and keloid (keloid). An automated keloidal segmentation model will be trained under the supervision of the segmented images.

3.3. Creation of a division Module Automatically

Studies have shown that vision converters are inference networks characterized by dense biases, requiring a substantial amount of training information. Nevertheless, there are not many training data in this study, thus before to training, a well-trained weight is required. Rather than utilizing the weight previously trained in the ImageNet directly, we utilize the Masked AutoEncoder (MAE) pretraining technique. Reconstructing the original image from each image using 75% of the mask patch as input is the aim of the training process. The model learns rich concealed data and infers complex reconstructions using this pretraining strategy. We utilised 1600 pretraining periods in line with the stated methodology.

After resizing the photos to 512 x 512, they are divided into 16 x 16 patches. As a result, each image generates 1024 patches in total. The segmentation decoder was an upernet, while the encoder was a VIT with 12 layers. A neural network was trained to function as a specialist and divide the keloid independently with the use of manual annotations. The model was written using PyTorch, and data augmentation techniques included random rigid rotation of 15 degrees and random flips in the horizontal and vertical axes. Backpropagation was performed using the SGD optimizer, and the learning rate was progressively reduced from 0.02. Using a single 3090 Nvidia GPU, the training procedure took two hours with a total of 100 epochs.

3.4. The Blood-Perfusion Analysis Module's development

The LSCI's capacity to produce a heat map of the bloodperfusion image that ranges from blue to red allows us to infer the blood-perfusion values for each pixel, even though we could have difficulties incorporating the software into the equipment used to take the initial blood- flow photosWe developed a mapping algorithm that links the RGB values of the image with the appropriate blood-perfusion values through matching the colour spectrum to the blood- perfusion value. Additionally, by cropping the plasma flow picture according to the outcomes of the automated categorization, we calculated the average blood-perfusion readings for the keloid area. By contrasting the blood-perfusion value that was first found in LSCI with the blood-perfusion value that was separately determined, the proportion of perfusion error was calculated.

3.5. Creation of the Assessment Section

We refrained from employing the mean blood-perfusion value for a direct evaluation of the keloid's growth state. This is because the blood circulation within a keloid is contingent on its inherent development state and because keloids frequently display an irregular perfusion distribution. Instead, the segmentation result was employed to mask the blood perfusion picture, eliminating any superfluous blood perfusion before resizing it to 512 512. Simultaneously, the blood-perfusion were generate 1024 images, each measuring 16 by 16. The images showing blood perfusion were encoded using a vision transformer.

Only patches with blood flow were supplied to the transformer to eliminate superfluous regions and reduce memory expenses. Following the perfusion encoding process, the perfusion parameters and intensity data from the intensity encoder were combined. Three classification predictions were generated when the combined feature was decoded using a forecasting decoder consisting of four transformer layers: progressive, steady, and regressive. Depending on whether the keloid got bigger, smaller, or remained identical in size over the previous year, patients reported three different keloid growth stages [5].25% of the pixels were randomly erased during the training process, which was carried out automatically. In 50, 100, and 200 epochs, the original acquisition rate of 0.001 was halved. Using a 3090 Nvidia GPU, this training process required roughly two hours and 400 drill epochs.

3.6. Creating the Matrix for Workflow and Valuation

The objective of this research was to improve the diagnostic and automated functionalities of the keloids assessment and treatment method in clinical environments, as illustrated in Figure 1. This experiment involved the development of three diagnostic components: an assessment module, a module for monitoring blood perfusion, and an automated segmentation module. The entire process was a cascaded vision transformer-based, semi-automated diagnosing approach. The patient's blood-perfusion and unlabeled intensity images must be manually collected and input into the computer's segment module before the keloid can be segmented. Ultimately, the keloid growth condition was ascertained by combining the evaluation module with the previously encoded intensity data and the clipped blood-perfusion image.

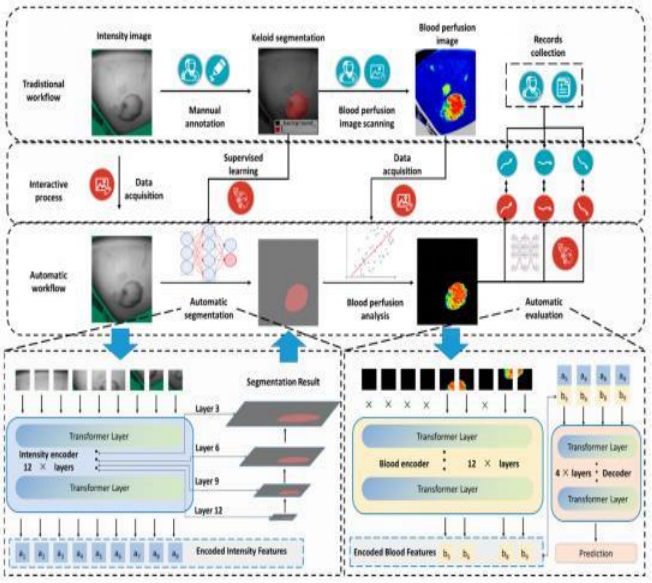

Figure 1. AI segmentation and evaluation workflow

5-fold cross-validation was used to independently train and validate the modules developed in this work. We chose a separate evaluation function for every method. We employed the DICEs assessment criterion for the automated segmentation module. The findings of automatic segmentation are more fecurate the higher the DICE score.

A & B stand for the manually drawn and deep learning features separated outputs that need to be evaluated, respectively.

$$DICE = \frac{2\,|A \cap B|}{|A| + |B|} \quad (1)$$

We employed the relative blood-perfusion differential and the perfusion error in blood to assess the variation in blood perfusion.

$$\text{perfusion blood error} = |A\text{-}B| \quad (2)$$

Relative perfusion blood error

$$= (|A\text{-}B|)/(\max([A],[B]) \times 100\% |A\text{-}B| \quad (3)$$

A and B stand for the blood-perfusion values that were derived from the blood-perfusion module and the original LSCI, respectively. We provided the Youden index, accuracy, sensitivity, and specificity for every category in the final evaluation analysis.

The research paper proposes a novel Multilayered ResNet50 architecture for keloid classification in medical imaging. The model enhances the ResNet50 architecture by introducing additional convolutional layers and adaptive filters, aiming to capture intricate features crucial for keloid identification. The formulation of the model includes a modified ResNet50 base with W layers and skip connections, augmented by M added convolutional layers denoted by Cm. The input to the model is xi, representing a keloid image. The output vi is a binary classification that indicates the existence or absent of a keloid. The suggested architectural representation in mathematics is described as follows: $hi+1 = F(hi,\theta i) = \sigma(\Sigma\ m = 1MWm * hi+bm)$ (4)

where σ is the activation function, Wm and bm are the weights and biases of the added convolutional layers, and θi, represents the set of parameters for the i-th layer. The final layer's output is computed as:

$$yi=softmax(hw + м) \quad (5)$$

The softmax function normalizes the output into probabilities, facilitating binary classification. Experimental results demonstrate superior performance compared to standard ResNet50 models, validating the effectiveness of the proposed Multilayered ResNet50 for accurate keloid classification in medical imaging.

4. Experimental Results

4.1. Study Samples

This study involved the enrollment of 150 keloids in total. The average age of the 75 men and 75 women was 30.6±11.1 years, the mean blood-perfusion was 129.9±41.0 and the mean keloid period was 7.1±3.9 as indicated in Table 1. In the regressive stage, there were 49 (32.7%) keloids, in the stable stage, there were 37(24.7\%). and in the progressive stage, there were 64 (42.7%).

There were big differences in blood perfusion at different places. The highest mean blood-perfusion measured by keloids on the face was 182.8±23.0~PU while the lowest mean bloodperfusion measured by keloids on the hip was 103.0±40.2~PU.

Table 1. Features of the Demo

Location	N	Male	female	Age	periods	perfusion	regressive	stable	progressive
Back	35	19	17	33.5±11.5	7.7±3.8	128.6±44.7	11	10	16
Chest	64	30	35	30.5±13.3	6.9±4.2	136.8±36.6	15	17	34
Ear	9	5	5	27.9±11.3	6.2±5.2	158.8±41.8	2	4	5
Face	7	5	3	28.8±4.7	9.8±4.2	182.9±27.0	1	2	6
Hip	10	6	5	35.2±9.8	6.1±3.2	104.0±43.2	8	2	2
Limb	19	9	11	33.3±11.4	6.8±4.2	106.2±39.4	13	4	4
Abdomen	13	8	6	30.3±9.2	8.1±4.4	117.5±35.7	6	5	4
All	151	76	76	32.6±12.1	7.2±3.8	128.9±45.0	50	38	65

4.2. Segmenting evaluation

The DICE value mean was calculated for each of the five training procedures following a five-fold instruction delivery. In the end, the suggested approach resulted in an average DICEs range of 0.905. Illustrations of the division process can be observed in Figure 2.

The original format of the brightness image is presented in the first column, manually annotated in the second column, and automatically segmented findings are showcased in the third column. It is demonstrated that compared to the manual segmentation border, the machine-generated segmentation boundary is smoother and more regular.

Studies on ablation between architectures and pretraining techniques were been out (Table 2 segmentation). It was concluded that the baseline techniques were hrnet and resnet. CNN and VIT, however, performed similarly when employing ImageNet pretraining weights (HRnet-c1 0.985 vs. VIT 0.890). With a DICE

value of 0.895, VIT's and when MAE was employed as the pretraining strategy, It beat CNNs by 2%.

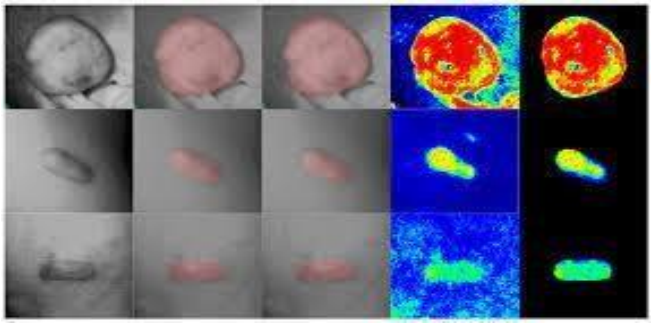

Figure 2.Results of segmenting and cropping the suggested modules. In this graphic, First are the original intensity photos; second are the manual annotations; third are the automatic segmentation; fourth are the original blood-perfusion images; and fifth are the cropped blood-perfusion.

Table 2.study of ablation

techniq ues	Pretrai ning	DICEs	techniq ues	Pretrai ning	Acc
Resnet 50supernet	-	0.751	M-Resnets 50	-	0.973
HRnet-cls	-	0.681	Resnets 101	-	0.903
Resnet 50supernet	ImageNet	0.871	Resnet 50	ImageNet	0.927
HRnet-cls	ImageNet	0.865	Resnets 101	ImageNet	0.933
VITsbaseupernet	-	0.672	Cascad es-VIT	-	0.897
VITsbaseupernet	ImageNet	0.890(0.025	Cascad es-VIT	ImageNet	0.914(+ 0)
VITsbaseuperne	MAEs	0.985(+0. 030)	+patche s selectio n	ImageNet	0.937(+ 0.014)

Note: The best outcome for each activity is displayed in bold language.

4.3. Perfusion Segment

Blood perfusions have been intended using manually produced blood-perfusion photographs and the results of the computerized segmentation.

The cropped image, which eliminates the skin pigmentation effect, is shown in the last column of Figure 2.

Comparative perfusion error was 7.8% ± 6.6% and the least mean flow error was 8.6 ± 5.4 PU, indicating exceptional precision for the proposed blood-perfusion module.

4.4. Final Evaluation

Following the division of the images into patches and the application of segmentation to mask the blood-perfusion image, the characteristics were stored with the blood characteristics. The final forecast was based on both intensity features and blood features. The automatic assessment module produced good prediction accuracies, according to the results. The Youden index, accuracies, specificities, and sensitivities were shown in Table 3. The three stages had sensitivity values of 0.936, 0.892, and 0.939. The three stages had specificities of 0.9 0,965, and 0.964, in that order. A mean precision of 0.927 was reported by the assessment module.

Table 3. The assessment of the module's outcomes

	REGRES SIVE	STABLE	PROGRE SSIVE	OVE RAL L
SENSITIVE	0.937	0.902	0.969	
SPECIFICA TIONS	0.971	0.995	0.974	
YOUDEN	0.907	0.886	0.924	
ACC	0.963	0.957	0.935	0.940

Based on ablation research, DL -based techniques may attain 0.89 accuracy even in the absence of pretraining, suggesting that predicting the development state is a reasonably simple task. CNNs also performed better than VIT in the absence prior to training (Resnet101 0.963 vs. VIT 0.887). Proposed work performed 1.4% better than CNNs after applying patch selection and concatenated (Resnet101 0.913 vs. VIT 0.927).

5. Conclusions

This research introduced a method for examining the phases of keloid development through the application of Laser Speckle Contrast Imaging (LSCI) using a Multi-layered ResNet50 architecture. The procedure comprised three components: an automated segmentation module, a module for measuring blood perfusion, and an assessment module. Utilizing the automated segmentation technique, we successfully segmented and identified the keloid, achieving a DICE score of 0.895. We manually specified the image to detect the blood perfusion zone within the keloid, using received blood perfusion images and automatic segmentation results. We then calculated the average blood circulation significance, whigh yielded an absolute error of 7.8% ± 6.6% and a mistake of 8.6 ±54 PU. We separated the blood perfusion pictures into patches and sent them to the assessment component in order to evaluate the growth status. In the end, our average accuracy came out to be 0.963. Division, evaluation, and evaluation are all combined in our developed workflow, which can facilitate and expedite the keloid assessment procedure in later clinical practice.

References

[1] Kulurkar, P., kumar Dixit, C., Bharathi, V. C., Monikavishnuvarthini, A., Dhakne, A., & Preethi, P. (2023). Al based elderly fall prediction system using wearable

sensors: A smart home-care technology with IOT. Measurement: Sensors, 25, 100614.

[2] Punarselvam, E., Sikkandar, M. Y., Bakouri, M., Prakash, N. B., Jayasankar, T., & Sudhakar, S. (2023). Retraction Note to: Different loading condition and angle measurement of human lumbar spine MRI image using ANSYS. 14. Punarselvam. E.. Devi, T. K., Britto. A., Prakash, N. B., & Suresh, P. (2020).

[3] Palanisamy, P., Padmanabhan, A., Ramasamy, A., & Subramaniam, S. (2023). Remote Patient Activity Monitoring System by Integrating IoT Sensors and Artificial Intelligence Techniques. Sensors, 23(13), 5869.

[4] Afza, F.; Sharif, M.; Khan, M.A.; Tariq. U.: Yong, H.-S.; Cha, J. Multiclass Skin Lesion Classification Using Hybrid Deep Features Selection and Extreme Learning Machine. Sensors (2022),22,799.

[5] Manzoor, K.; Majeed, F.; Siddique, A.; Meraj, T.; Rauf, H.T.; El-Meligy, M.A.; Sharaf, M.; Elgawad, A.E.E.A. A LightweightApproach for Skin Lesion Detection Through Optimal Features Fusion. Comput. Mater. Contin. (2022), 70, 1617-1630.

[6] Huang. S.; Dang. J.; Sheckter, C.C.; Yenikomshian, H.A.; Gillenwater, J. A systematic review of machine learning and automationin burn wound evaluation: A promising but developing frontier. Burns (2021), 47, 1691-1704.

[7] Zhu, C.-Y.; Wang, Y.-K.; Chen, H.-P.; Gao, K.-L.; Shu, C.; Wang, J.-C.; Yan, L.-F.; Yang. Y-G.; Xie, F.-Y.; Liu, J. A Deep LearningBased Framework for Diagnosing Multiple Skin Diseases in a Clinical Environment. Front. Med. (2021), 8, 626369.

[8] Asokan, R., & Preethi, P. (2021). Deep learning with conceptual view in meta data for content categorization. In Deep Learning Applications and Intelligent Decision Making in Engineering (pp. 176-191). IGI Global.

[9] Yang, C.-H., Ren, J.-H.; Huang, H.-C.: Chuang, L.-Y.; Chang, P.-Y. Deep Hybrid Convolutional Neural Network for Segmentationof Melanoma Skin Lesion. Comput. Intell. Neurosci. (2021), 2021,9409508.

[10] Dong, Y.; Wang, L.; Cheng, S.; Li, Y. FAC-Net: Feedback Attention Network Based on Context Encoder Network for Skin LesionSegmentation. Sensors(2021), 21, 5172,

[11] Punarselvam, E., Sikkandar, M. Y., Bakouri, M., Prakash, N. B., Jayasankar, T., & Sudhakar, S. (2021). Different loading condition and angle measurement of human lumbar spine MRI image using ANSYS. Journal of Ambient Intelligence and Humanized Computing, 12, 4991-5004.

[12] poldovanu, S.; Michis, F.A.D.; Biswas, K.C.; Culea-Florescu, A.; Moraru, L. Skin Lesion Classification Based on Surface FractalDimensions and Statistical Color Cluster.Features Using an Ensemble of Machine Learning Techniques. Cancers (2021), 13, 5256.

[13] Yao, P.; Shen, S.; Xu, M.; Liu, P.; Zhang, F.; Xing, J.; Shao, P.; Kaffenberger, B.; Xu, R.X. Single Model Deep Learning on ImbalancedSmall Datasets for Skin Lesion Classification. IEEE Trans. Med. Imaging 2021, 41,1242-1254.

[14] Chen, C.; Zhang, M.; Yu, N.; Zhang, W.; Long, X.; Wang, Y.; Wang, X. Heterogeneous Features of Keloids Assessed by Laser Speckle Contrast Imaging: A Cross-Sectional Study.Lasers Surg. Med. (2020), 531865-871.

[15] Preethi, P., & Asokan, R. (2020, December). Neural network oriented roni prediction for embedding process with hex code encryption in dicom images. In Proceedings of the 2nd international Conference on Advances in Computing, Communication Control and Networking (ICACCCN), Greater Noida, India (pp. 18-19).

[16] Punarselvam. E.. Devi, T. K., Britto. A., Prakash, N. B., & Suresh, P. (2020).Segmentation Analysis Techniques and Identifying Stress Ratio of Human Lumbar Spine Using ANSYS. Journal of Medical Imaging and Health Informatics, 10(10), 2308-2315.

[17] Amin, J.; Sharif, A.; Gul, N.; Anjum, M.A.; Nisar, M.W.; Azam, F.; Bukhari, S.A.C. Integrated design of deep features fusion forlocalization and classification of skin cancer.
Pattern Recognit. Lett. (2019), 131,63-70.

[18] Uetake, H. Novel assessment tool based on laser speckle contrast imagingto diagnose severe ischemia in the lower limb for patients with peripheral arterial disease. Lasers Surg.

Med. (2017), 49, 645-65.

[19] Ronneberger, O.; Fischer, P.; Brox, T. U-Net: Convolutional networks for biomedical image segmentation. In Medical

Image Computingand Computer-Assisted Intervention-
MICCAI 201: Springer International Publishing: Cham,

Switzerland, (2015); pp. 234-241.

[20] Roustit, M.; Cracowski, J.-L. Non-invasive Assessment of
Skin Microvascular Function in Humans: An Insight Into

Methods. Microcirculation (2011) 19, 47-64.